Available online at www.sciencedirect.com

ScienceDirect

Procedia Manufacturing 3 (2015) 1379 – 1386

Procedia MANUFACTURING

6th International Conference on Applied Human Factors and Ergonomics (AHFE 2015) and the Affiliated Conferences, AHFE 2015

Towards a robotic knee exoskeleton control based on human motion intention through EEG and sEMGsignals

A.C.Villa-Parra[a,b], D.Delisle-Rodríguez[a,c], A. López-Delis[c], T. Bastos-Filho[a,*], R. Sagaró[d], A. Frizera-Neto[a]

[a]*Post-Graduate Program in Electrical Engineering, Universidade Federal do Espírito Santo, Vitória,Brazil*
[b]*GIIB, Universidad Politécnica Salesiana, Cuenca, Ecuador*
[c]*Center of Medical Biophysics, Universidad de Oriente, Santiago,Cuba*
[d]*Mechanical and Design Engineering Department, Universidad de Oriente, Santiago,Cuba*

Abstract

The integration of lower limb exoskeletons with robotic walkers allows obtaining a system to improve mobility and security during gait rehabilitation. In this work, the evaluation of human motion intention (HMI) based on electroencephalogram (EEG) and surface electromyography (sEMG) signals are analyzed for a knee exoskeleton control as a preliminary study for gait neuro-rehabilitation with a hybrid robotic system. This system consists of the knee exoskeleton H2 and the UFES's Smart Walker, which are used to restore the neuromotor control function of subjects with neural injuries. An experimental protocol was developed to identify patterns to control the exoskeleton in accordance with the HMI-based on EEG/sEMG. The EEG and sEMGsignalsare recorded during thefollowing activities: stand-up/sit-down and knee flexion/extension. HMI is analyzed through both event-related desynchronization/synchronization (ERD/ERS) and slow cortical potential, as well as the myoelectric patternclassification related to lower limb. The feature extraction from sEMG signals is based on vector combinations in time and frequency domain which are used for a pattern classification stage trough an artificial neural network with LevenbergMarquadt training algorithm and support vector machine. Preliminary results shown that a combination of EEG/sEMG signals can be used to define a control strategy for the robotic system.

Peer-review under responsibility of AHFE Conference

*Keywords:*Human-motion-intention;Knee exoskeleton; Pattern recognition; EEG; sEMG

* Corresponding author. Tel.: +552740092077; fax: +552740092644.
E-mail address: teodiano.bastos@ufes.br

Peer-review under responsibility of AHFE Conference
doi:10.1016/j.promfg.2015.07.296

1. Introduction

Robotic devices applied in rehabilitation training have advantages over conventional therapies because the user increases his/her motivation to train and the opportunity for executing exercise independently in order to improve the quality of training and level of motor recovery[1]. For gait rehabilitation, exoskeletons and smart walkers are widely employedwith promising results. The exoskeletons are portable devices that provide mobility and can achievenormal gait kinematics. These devices are effective in clinical applications for paraplegics and, significantly reduce the metabolic cost and increase the walking speed[2].The robotic walkers are used in physiotherapy because can avoid muscular atrophy by forcing the user to make some movement and provide balance and physical support. Examples of exoskeletons are the Vanderbilt lower limb exoskeleton for providing legged mobility to paraplegics[3]; the Hybrid Assistive Limb (HAL), cited as the first exoskeleton employed in hospitals for rehabilitation.Examples of smart walkers are GUIDO smart walker with a system to detect obstacles and advertise collision risk[4]; and the UFES's smart walker (USW) to provide safety and a more natural human gait[5]. The integration of exoskeletons with control based on EEG/sEMG signals with robotic walkers is a tendency to obtain a system for gait neuro-rehabilitation because can provide advantages of better controllability [6].

Nowadays, researches about gait neuro-rehabilitation systems are based on human motion intention (HMI) detection [7], [8]. Electroencephalogram (EEG) signals and surface electromyography (sEMG) signals provide physiological information about HMI and the currenttrend is to develop hybrid control methods where the couplingof thesebiosignalscan be used to enhance the performance of the controller based on HMI [9]. Also, HMI recognition can be usedtodeterminate the torque to be supplemented by the exoskeleton actuator in the pathological gait [10]. The current researches through sEMG signals predict the HMI for exoskeleton control that can be adjustable based on human-robot interaction improving the rehabilitation training [11].On the other hand, EEG signals have been explored very little in the control of lower limbs[12]. In neuro-control applications, bioelectrical potentials measured from the brain on primary motor areas and supplementary motor cortex have demonstrated high potentialities to stroke treatment a Brain Computer Interface (BCI) in neuro-rehabilitation applications [1].

The goal of this work is to analyze theHMIbased on EEG/sEMG from some daily activities related to knee motion in order to define in future worksa control strategy for a robotic system during gait rehabilitation using a residual motor skill of user.The following sections present the details of the robotic system proposed with their control strategy, then the experimental protocol used to acquire the EEG/sEMGsignals to identify patterns to control the knee exoskeleton based onHMI.Finally, the methods based on event-related desynchronization/synchronization (ERD/ERS) and slow cortical potential (SCP) from EEG signals,the feature extraction and classification pattern from sEMG signals to analyze the HMI are presented, including the discussion of the results.

2. Materials and methods

2.1. Robotic system

The system consists of a robotic knee exoskeleton (KE)(model EXO-H2[13])and the USW[5]integrated with a EEG and sEMG acquisition equipment[14], as well as proprioceptive sensors as footswitch, goniometerand infrared laser.Fig. 1 shows the block diagram of the robotic system based on HMI for gait rehabilitation. The KE supplies assistive torque at the knee to alleviate the loading and reduce the excessive muscular effort to perform sessions for gait rehabilitation and to assist in daily activities. The USW is the combination of a conventional walker with a Pioneer 3DX robot (manufactured by Adept), which can guide the users during the therapy sessionsand assist them to keep a stable posture during the gait [15]. The interaction USER–KE–USW allowsincreasing the stability during gait and provides safety for the user. The USW controller is based on the inverse kinematics of the human-walker model anda laser sensorallowrecognizethe leg position [15].During the gait, safety rules (SR) analyze risky conditions and guarantees safety for the user while using the system. The SR define a safe zone and the controller corrects the distance to keep the user inside of this area, which can be modified at any moment by the therapist [15].

A previous study[16] evaluated the assisted gait by USW in post stroke hemiparetic individuals. The study reports that the gait speed was decreased using the walker, and produce changes in the duration of the support phase of the gait cycle[17]. In this condition, part of the user´s weight is transfer to the ground thought the USW and the weight

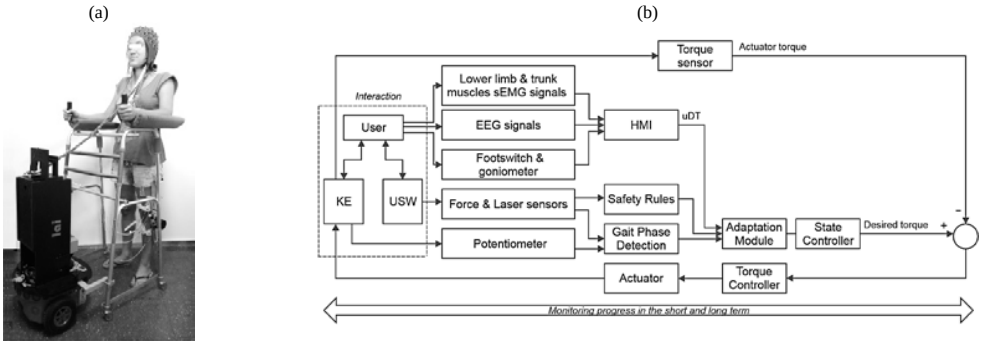

Fig. 1. (a) Interaction USER–KE–USW; (b)Block diagram of USER–KE–USW based-on HMI for gait rehabilitation.

carried through the KE is reduced during stance phase, as the case where crutches are used [18]. In that instance, the KE torque controller requires both robust gait phase detection and user developed torque (uDT) during the KE–USER–USW walking, in order to adapt different torques during stance and swing phase.

With the data of HMI, it is possible to infer control outputs that make the user's gait more natural and helps in the rehabilitation process, making this system suitable to be used in physiotherapy sessions. The HMI module (see Fig.1) determines the motion state using support vector machine (SVM) and artificial neural network (ANN) based on sEMG signals from the lower limb and trunk muscles responsible for the knee motion during walking [19]. The relevant information of EEG signal correlated with planning movement [20]was considered for the HMI recognition, through both event-related ERD/ERS and SCPs. For the KE control, the uDT estimation is realized with a torque estimation algorithm as part of the adaptive module, which is based onHMI information, the gait phase detection and also SR from the USW. The uDT allowsidentifying the motion class of the user, which defines the torque through a state-controller based on finite state machine [21].

The monitoring task, which is based on the use of sensors of the KE-USW, is carried out in order to have a complete evolution of the users and to get measurement of active time of rehabilitation.

2.2. Experimental Procedure

Four health subjects (male) participated and provided informed consent. Fig. 2 shows the eighth motion-class recorded during the experimental protocol to analyses the HMI. The subjects were cued to perform each trial through a sound stimulus with a period of 10 s, and each condition has 60 trials with a rest of 3 min. The BrainNet BNT 36 equipment was used to measure the sEMG and EEG signals from 10 to 100 Hz and 0.1 to 100 Hz respectively, with frequency rate of 400 Hz. The levels C7, T3, T7, T12 and L4 were used in the lumbar *erector spinal* (ES) muscle and theright lower limb muscles: the *rectus femoris*(RF), *vastuslateralis*(VL), *biceps femoris*(BF), *semitendinosus* (S) and *gastrocnemius* (G). Two pairs of 10 mm Ag/AgCl surface electrodes are located in bipolar configuration over the muscleswith a distance of 3–5 cm between the centers of each pair. The position of reference electrode is on the right leg. The EEG signals were measured from electrodes FC3, FC1, FCz, FC2, FC4, C5, C3, C1, Cz, C2, C4, C6, CP5, CP3, CP1, CPz, CP2, CP4, CP6 and Pz, using the 10-20 international system. The reference electrodes were located on Cz, earlobes A1&A2, and on the forehead aligned with FPz electrode (between the eyebrows).

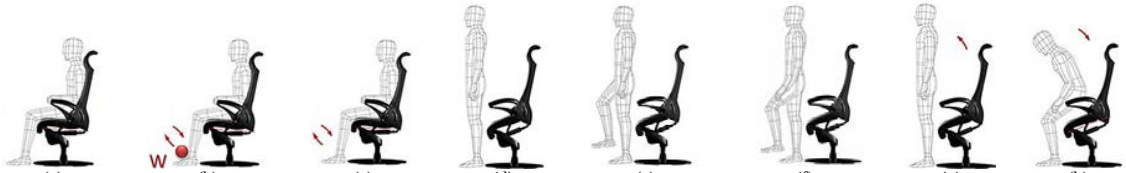

Fig. 2. Motion-classes:(a) Rest in sitting position; (b) knee flexion-extension with weight; (c) knee flexion-extension; (d) rest in standing position; (e) right leg flexion-extensionin standing position; (f) left leg flexion-extensionin standing position; (g) stand-up; (h) sit-down.

2.3. Onset/Offset motion intention detection

sEMG signal measured from RF was used to obtain the reference time of knee motion onset/offset. First, atrigger signal correlated to each sound stimulus aforementioned was used to align the sEMG epochs (from –3 to 10 s) related to the same test. Second, sEMG epochs were normalized, and pre-processed through a bandpass filter (Butterworth, 2nd order) from 10 to 100 Hz. Third,sEMG epochs were smoothed to obtain a linear envelope through the sample entropy (SampEn) method[22]and a lowpass filter (Butterworth, 2nd order) of 7 Hz [17]. In this study, the values $m = 2$ and $r = 0.25 \times SD$were used, such as in [22].Finally, the envelopes were averaged to compute a threshold value from the baseline noise, which are used to determine the onset/offset of the muscular activation. Mean values were computed through a sliding windows of 2 s and overlapping of 0.5 s, which were averaged to obtain a threshold value (5 % > the mean value), before and after the peak value of the envelope signal.

In this work, LAR and WAR filters were used to reduce the common interference throughout the EEG signals. These methods are recommended in motor task applications, [23], andallow converting the reference-dependent raw in reference-free data, which can be used to obtain maps with more focus pattern.LAR filter (see equation 1) improves the Laplacian method, where the signals of a set electrodes surrounding a center electrode are averaged taking into account the current distances between electrodes [23].

$$V_i^{LAR} = V_i^{CR} - \sum_{j \in S_i} g_{ij} V_j^{CR}, \; g_{ij} = \frac{1}{d_{ij}} \left(\sum_{j \in S_i} \frac{1}{d_{ij}} \right)^{-1}, \tag{1}$$

whereS_i is the set of surrounding electrodes for source electrode V_i^{CR}, d_{ij} and g_{ij} are the distance and weight index between electrodes i and j. Both LAR-small and LAR-large use the nearest and next neighbor electrodes respectively, [23]. In this work, all neighbor electrodes were considered to both methods. WAR filter (seeequation (2)),is a modification of common average reference, whichit is consider the actual distances between electrodeswhere N is the number of electrodes.

$$V_i^{WAR} = V_i^{CR} - \sum_{j=1}^{N} g_{ij} V_j^{CR}, \; g_{ij} = \frac{1}{d_{ij}} \left(\sum_{\substack{j=1 \\ j \neq i}}^{N} \frac{1}{d_{ij}} \right)^{-1} \tag{2}$$

The ERD/ERS potentials are used to obtain the movement onset/offset respectively.*ERD/ERS* reflect changes in the activity of local interactions between main neurons and interneurons that control the frequency components of the ongoing EEG during motor tasks [24]. Voluntary movements result in a circumscribed desynchronization in the upper alpha (10 to 12 Hz) and lower beta (19to 24 Hz) bands, located close to sensorimotor areas [24]. This desynchronization starts about 2 s prior to movement onset over the contralateral Rolandic region and becomes bilaterally symmetrical immediately before movement execution [24]. A foot area mu ERD located close to the primary foot area between both hemispheres is less frequent, however with a lower beta band it is possible to obtain a focused pattern around the primary foot area [24]. On the other hand, an oscillating brain signal with a good signal-to-noise ratio (post-movement beta ERS) is found in the first second after termination of a voluntary movement. This low amplitude activity is located with a focus around the corresponding sensorimotor representation area [24], which can be found from 14 to 18 Hz, and 26 to 30 Hz (higher beta band) bands. The ERD/ERS potentials are computed through the following steps: 1) bandpass filter; 2) calculation of the point to point of inter-trial variance; 3) averaging over time [24]. The subject-specific frequency band was computed through the continuous wavelet transform for scale factor from 8 to 70 [24]to analysis the ERD/ERS potentials [24]. The ERD/ERS maps are computed on the original data for aforementioned pre-processing methods based on Euclidean distance. The percentage of ERD or ERS is computed prior the activation onset of RFmuscle from 2.0 to –0.5 s through the equation (3), where A is the power and R is the baseline or reference period.

$$ERD\% = 100(A - R)R^{-1}, \tag{3}$$

In this study, *SCP* is analyzed in the frequency range of 0.1 to 1 Hz, which is reported to better capture of the anticipatory-related SCPs [25]. SCP is obtained through the following steps: 1) 4 s of analysis epochs from -3 to +1 s respect to the activation of RF muscle (onset reference) are cut from the raw data in an off-line manner; 2) the epochs are filtered by a lowpass filter with a cut frequency of 1 Hz, and smoothed through a linear detrend filter to remove the inappropriate occurrence trend; and 3) EEG epochs are aligned to the onset reference and averaged. The EEG baseline is defined as the mean amplitude of the first 0.4 s of the epoch [25].

2.4. HMI recognition from sEMG

sEMG signals measured in the lower limb were analyzed using a combination of features in time and frequency domains, which are used for pattern classification through an ANN and SVM. Before the feature extraction (FE) and classification process, sEMG data were normalized to provide a common basis of comparison across different sessions and different muscles. In this case, a common reference was adopted from the minimum and maximum sEMG values. In the time domain, the mean absolute value (MAV) and waveform length (WL)[26]were used as features. MAV provides the average amplitude of the x_i as show in equation (4), where x_i is the amplitude value of sample *i*of sEMG segment, and*N*represents the total sample. WL provides the cumulative length of the waveform over the time segment, see equation (5). In the frequency domain, an auto-regressive (AR) model was implemented by equation (3), where *P* represents the order of the AR model and w_i the white noise error. The coefficients $a_p$of the AR model contain information about the sEMG pattern.

$$MAV = \left(1/N\right)\sum_{i=1}^{N}\left|x_i\right|, \tag{4}$$

$$WL = \sum_{i=1}^{N-1}\left|x_{i+1} - x_i\right|, \tag{5}$$

$$x_i = \sum_{p=1}^{P} a_p x_{i-p} + w_i, \tag{6}$$

For different muscle contraction modes different sets of parameters are identified. The model is supported by the Levinson–Durbin recursive method based on the autocorrelation matrix [26]. The four-order auto-regressive model was defined to obtain the linear prediction coefficients because allows representing the signal as a temporal series [26]. Each sEMG channel and theirs feature vectors were concatenated from the first four auto-regressive coefficients with MAV and WL values, resulting 30 coefficients (5 channels × 6 features vectors/channel) for lower limb muscles.For *myoelectric pattern classification*, two classification methods ANN and SVM were applied to discriminate the eight motion-classes from sEMG feature vectors. The Levenberg-Marquardt (LM) algorithm is used toANN training, which is very efficient for training moderate-sized feed-forward ANN[27]. SVM is a kernel-based approach with a strong theoretical background, and is a tool for machine learning tasks. SVM classifier [28] takes into account the input data as an *n*-dimensional feature space, then an $(n - 1)$ dimensional hyperplane separates the space into two parts. The high generalization and classifying linearly-inseparable patterns with small computational complexity of SVMare useful for real-time applications and for classifying sEMG signal patterns because theirs features change throughout time and can allow real-time motion classification, respectively [28].

The LM network has a structure of three layers with thirty input nodes, sixty nodes in the second layer (associated with tangential functions)and one node in the output layer (associated with a linear function) that represents one of the eight motion classes.The same initial weight values were used for all three layers (zero for all neurons). A total of 50 iterations wasadopted, withmean squared error (MSE) stop criterion of 10^{-25} n.u.^{2}, and the initial learning rate of 0.05. This structure was chosen empirically, based on experiments aimed at minimizing the MSE. For the SVM classifier a radial basic function (RBF) kernel suggested for uses in myoelectric pattern recognition applications was configured.The regularization parameter was adjusted for C=10and the tolerance of the stop criterion was 10^{-5} n.u.^{2}. In the feature extraction, a window of 300 ms in length, shifted 150 ms for training and testing process, was used.The classifier's training and testing stages were implemented through the *k*-fold cross-validation technique,based on

Table 1. Subject specific frequency obtained from EEG channels with maximum ERD/ERS potentials value.

Subject	Knee extension/flexion				Stand-up				Sit-down			
	ERD		ERS		ERD		ERS		ERD		ERS	
	LF	HF	LF	HF	LF	HF	LF	HF	LF	HF	LF	HF
1	19.04	24.32	15.74	19.74	19.04	24.18	16.45	20.45	19.04	24.49	16.62	20.62
2	19.04	24.33	16.68	20.68	19.04	24.32	16.82	20.82	19.04	24.28	16.43	20.43
3	19.04	24.23	16.95	20.95	19.04	24.28	16.37	20.37	19.04	24.49	18.06	22.06
4	19.04	24.26	16.94	20.94	19.04	24.24	16.38	20.38	19.04	24.41	17.62	21.62

LF: low frequency, Hz; HF: High frequency, Hz; ERD: Event-related desynchronization; ERS: Event-related synchronization

the partition of the k samples sub-conjunct.One sub-conjunct represents the testing data, and the rest (k−1) the training, where k = 10. For the implementation of the myoelectric pattern classifiers, information about the classes during the training process was used.The performance was analysed through the statistical indicators: total error rate (TER)of classification, sensitivity (SS), specificity (SP) and predictive positive value (PPV).

The algorithms were implemented in off-line mode, using functions provided by Matlab®.

3. Results

Table 1 shows the specific-subject frequency bands obtained from largest beta ERD/ERS during knee flexion-extension, stand-up and sit-down. All subjects show a largest beta ERD around 20 to 24 Hz band, as well as a largest beta ERS around 16 to 22 Hz, focused closely to the primary foot area between both hemispheres. Similar results were reported in [24], where a higher focused pattern of ERD/ERS potential was obtained in the 20 to 24 Hz band during foot movement.Fig. 3 shows a largest beta ERD/ERS around primary foot area to three activities with knee movements of the subject 4. The largest beta ERD patterns was obtained to stand-up and sit-down, which can be related to task complexity [24]. ERD/ERS potentials more focused to primary foot area was obtained to WAR method, asimilar results are presented in [23]. However, we consider that an adaptive spatial filter should be explored to improve the focus area of ERD/ERS, because the weight index of WAR method is based on the Euclidean distance between neighbor and source electrode, which is not sufficient to obtain the common interference from neighbor electrodes with good accuracy and precision. In motion applications,as gait analysis and rehabilitation, as well as the activities presented in this work, EEG signals can be affected by several sources of interference and artifacts, such as: electrode movements, eyes movements and blink potentials, myoelectric and cardiac activities, non-mu-rhythm of EEG components as the visual alpha rhythm, and others. Then, aforementioned

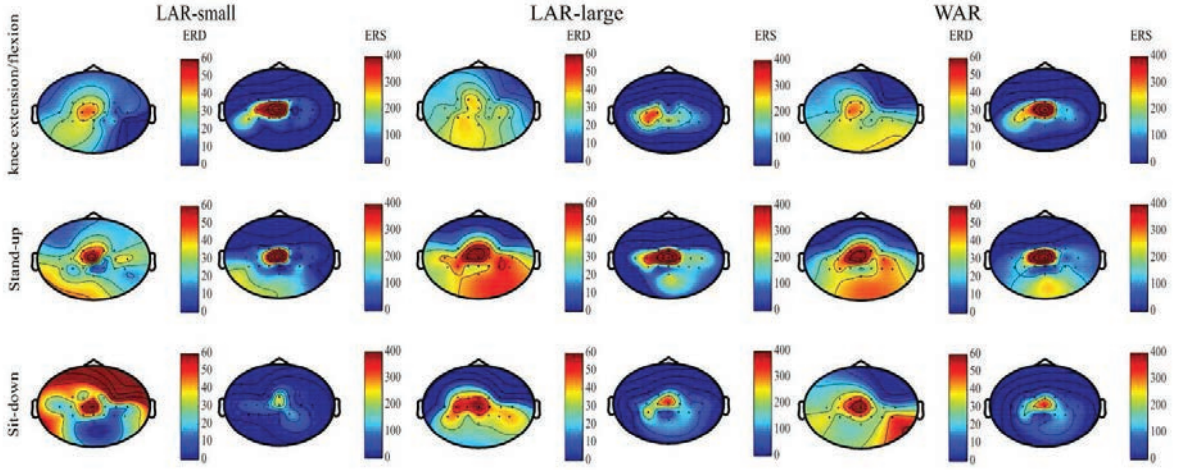

Fig. 3. ERD/ERS distribution computed in the subject 4. The top, middle and bottom rows are related to knee extension/flexion, stand-up from sit position and sit-down from up position, respectively.

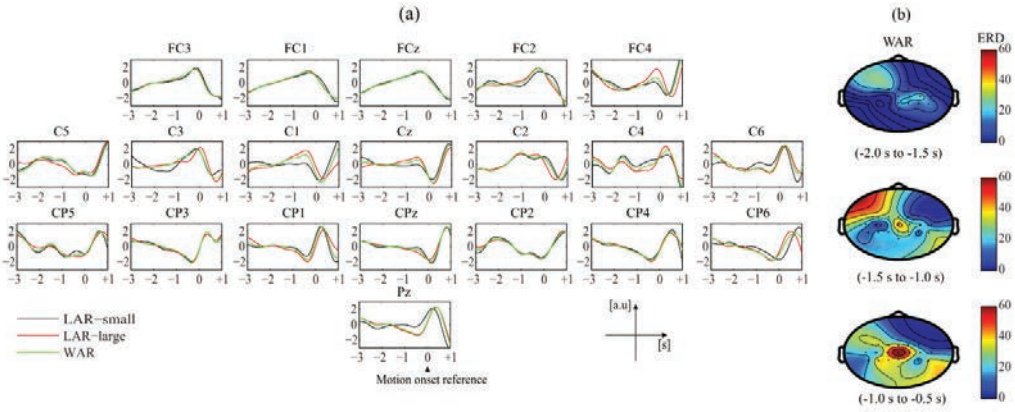

Fig. 4.Representation of SCP and ERD distribution obtained fromsubject 4 during sit-down activity: a) SCP waves obtained from EEG signals pre-processed through LAR-small, LAR-large and WAR spatial filters; b) ERD distribution computed from sliding windows of 0.5 s prior sit-down activity before pre-processing EEG signals with WAR method.

spatial filters based on Euclidian distance can contribute to add artifacts on source electrode, which are present in some neighbor electrode.The SCPs were obtained to sit-down activity before be application of the LAR-smallest, LAR-large and WAR spatial filters(see Fig. 4a). The ERD distribution computed from sliding windows of 0.5 s without overlapping from −2s to −0.5s prior sit-down activity from standing position is showed in Fig. 4b. In the first 0.5 s prior to sit-down activity, the left frontal cortical region (around FC3 and FC1 electrodes) and the right motor cortical region (C2 and C4 electrodes) show the largest beta ERD patterns. After, the largest ERD is more focused around primary foot area. The best waveforms of SCPs were obtained to electrodes located in the frontal cortical region and nearest to primary foot area. Previous reports showed that frontal lobe is largely concerned with planning future action and with the control of movement [29].

Regarding HMI recognition from lower limb sEMG,Fig. 5a presents a statistical comparison between the proposed classifiers. ANN classifier presents a best performance respect to SVM classifier related to TER, SS, SP and PPV quantitative metric, meaning a higher accuracy in recognition the eight motion-classes and robustness in presence of the positive and negative false during classification. The high specificity, sensibility and predictive values in both classifiers, show that the movement actions rate correctly accepted and rejected is satisfactory. Fig 5b presents the scatters plots based on the feature vectors from ANN classifier. The scatters plots present the feature vectors and the representative motion classes by the fifth myoelectric channels. From a qualitative evaluation, the classifier provides a good discrimination, based on MAV, WL and auto-regressive feature vectors.

4. Conclusions

The preliminaryanalysis ofthe HMI recognition related to the knee motion based on sEMG/EEG signalsshows that the proposed methods are suitable to define a control strategy for the KE inthe daily activities (motion-classes) considered in this study, in order to develop a system to restore the neuro-motor function of users with neural

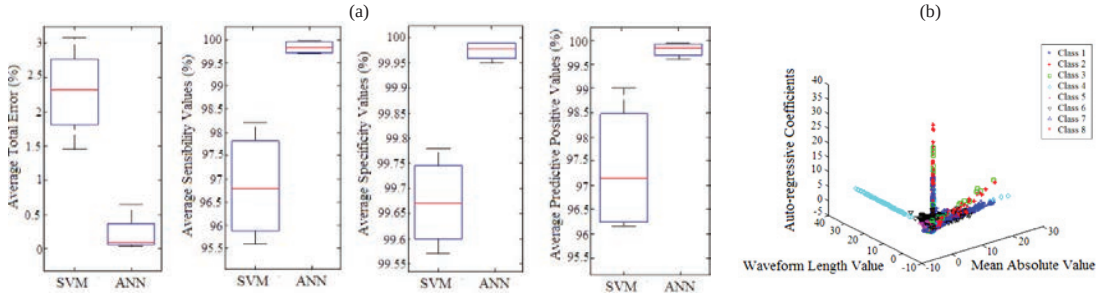

Fig. 5. (a) Statistical comparison between SVM and ANN classifiers; (b) Scatter plot the feature vectors from the ANN classifier.

injuries and muscular disabilities. HMI recognition and phase gait identification to define a KE control strategy from EEG and trunk muscles information will be explored in future works.

Acknowledgements

Authors would like to thank CAPES by support to this research. A.C.V. also thanks SENESCYT/ Ecuador.

References

[1]J.-M. Belda-Lois, S. M. Horno, I. Bermejo-Bosch, J. C. Moreno, J. L. Pons, D. Farina, M. Iosa, M. Molinari, F. Tamburella, A. Ramos, A. Caria, T. Solis-Escalante, C. Brunner, y M. Rea, «Rehabilitation of gait after stroke: a review towards a top-down approach», J. NeuroEngineering Rehabil., vol. 8, n.o 1, p. 66, dic. 2011.
[2]S. Viteckova, P. Kutilek, y M. Jirina, Wearable lower limb robotics: A review, Biocybern. Biomed. Eng., vol. 33, n.o 2, pp. 96-105, 2013.
[3]R. J. Farris, H. A. Quintero, S. Murray, K. Ha, C. Hartigan, y M. Goldfarb, A Preliminary Assessment of Legged Mobility provided by a Lower Limb Exoskeleton for Persons with Paraplegia, 2013.
[4]G. Lacey y D. Rodriguez-Losada, The Evolution of Guido, IEEE Robot. Autom. Mag., vol. 15, n.o 4, pp. 75-83, 2008.
[5]C. Valadao, C. Cifuentes, A. Frizera, R. Carelli, y T. Bastos, A Smart Walker to Help the Mobility of People with Disabilities and Elderlies, presentado en V Congreso Internacional de Diseño, Redes de Investigación y Tecnología para todos, 2013, pp. 12-20.
[6]K. Kong y D. Jeon, Design and control of an exoskeleton for the elderly and patients, Mechatron. IEEEASME Trans. On, vol. 11, n.o 4, pp. 428–432, 2006.
[7]J. Lobo-Prat, P. N. Kooren, A. H. Stienen, J. L. Herder, B. F. Koopman, y P. H. Veltink, Non-invasive control interfaces for intention detection in active movement-assistive devices, J. NeuroEngineering Rehabil., vol. 11, n.o 1, p. 168, dic. 2014.
[8]H. Zabaleta, M. Bureau, G. Eizmendi, E. Olaiz, J. Medina, y M. Perez, Exoskeleton Design for Functional Rehabilitation in Patients with Neurological Disorders and Stroke, in Challenges for Assistive Technology, Donosia, Spain., 2007, vol. 20, pp. 420-425.
[9]R. A. R. C. Gopura, D. S. V. Bandara, J. M. P. Gunasekara, y T. S., Recent Trends in EMG-Based Control Methods for Assistive Robots, in Electrodiagnosis in New Frontiers of Clinical Research, D. H. Turker, Ed. InTech, 2013.
[10]T. D. Lalitharatne, K. Teramoto, Y. Hayashi, y K. Kiguchi, Towards Hybrid EEG-EMG-Based Control Approaches to be Used in Bio-robotics Applications: Current Status, Challenges and Future Directions, Paladyn J. Behav. Robot., vol. 4, n.o 2, pp. 147–154, 2013.
[11]G. Chen, C. K. Chan, Z. Guo, y H. Yu, A review of lower extremity assistive robotic exoskeletons in rehabilitation therapy, Crit. Rev. Biomed. Eng., vol. 41, n.o 4-5, pp. 343-363, 2013.
[12]J. T. Gwin y D. Ferris, High-density EEG and independent component analysis mixture models distinguish knee contractions from ankle contractions, in 2011 Annual International Conference of the IEEE Engineering in Medicine and Biology Society,EMBC, 2011, pp. 4195-4198.
[13]Technaid, EXO-H2. 2014. Available: http://www.technaid.com/en/products/exoskeleton
[14]Delisle-Rodríguez, A. C. Villa-Parra, J. Castillo-García, Moraes, T. Bastos, Frizera Neto, y A. Lopez Delis, Development of an EEG and sEMG Wireless System for a Robotic Walker, in XXIV Congresso Brasileiro de Engenharia Biomédica – CBEB 2014, Uberlandia, Brasil, 2014.
[15]C. Valadao, F. Lotério, V. Cardoso, T. Bastos, A. Frizera Neto, R. Carelli, Robotic Walker to Assist and Monitor Physiotherapy Sessions, en Proceedings of the 1st International Workshop on Assistive Technologies, Vitória Brazil, 2015.
[16]F. Lotério, Análise do Padrão de Ativação Muscular de Indivíduos Hemiparéticos Pós-Avc em Marcha Assistida por Andador Robótico», UFES, Vitória Brazil, 2015.
[17]P. Konrad, The abc of emg, Pract. Introd. Kinesiol. Electromyogr., vol. 1, 2005.
[18]U. Onen, F. M. Botsali, M. Kalyoncu, M. Tinkir, N. Yilmaz, Y. Sahin, Design and Actuator Selection of a Lower Extremity Exoskeleton», IEEEASME Trans. Mechatron., pp. 1-10, 2013.
[19]J. R. Nymark, S. J. Balmer, E. H. Melis, E. D. Lemaire, y S. Millar, «Electromyographic and kinematic nondisabled gait differences at extremely slow overground and treadmill walking speeds, J. Rehabil. Res. Dev., vol. 42, n.o 4, pp. 523-534, ago. 2005.
[20]Y. Wang, B. Hong, X. Gao, y S. Gao, Design of electrode layout for motor imagery based brain–computer interface, Electron. Lett., vol. 43, n.o 10, pp. 557–558, 2007.
[21]B. Shen, J. Li, F. Bai, y C.-M. Chew, Development and control of a lower extremity assistive device (LEAD) for gait rehabilitation, in IEEE. International Conference on Rehabilitation Robotics: [proceedings], Seattle, Washington, 2013, vol. 2013, p. 6650367.
[22]X. Zhang y P. Zhou, Sample entropy analysis of surface EMG for improved muscle activity onset detection against spurious background spikes, J. Electromyogr. Kinesiol. Off. J. Int. Soc. Electrophysiol. Kinesiol., vol. 22, n.o 6, pp. 901-907, dic. 2012.
[23]D. G. Pfurtscheller, C. Neuper, y J. Berger, Source localization using eventrelated desynchronization (ERD) within the alpha band, Brain Topogr., vol. 6, n.o 4, pp. 269-275, jun. 1994.
[24]G. Pfurtscheller y F. H. Lopes da Silva, Event-related EEG/MEG synchronization and desynchronization: basic principles, Clin. Neurophysiol. Off. J. Int. Fed. Clin. Neurophysiol., vol. 110, n.o 11, pp. 1842-1857, nov. 1999.
[25]E. Lew, Detection of self-paced reaching movement intention from EEG signals, Front. Neuroengineering, vol. 5, 2012.
[26]M. Zecca, S. Micera, M. C. Carrozza, P. Dario, Control of multifunctional prosthetic hands by processing the electromyographic signal, Crit. Rev. Biomed. Eng., vol. 30, n.o 4-6, pp. 459-485, 2002.
[27]M. T. Hagan y M. B. Menhaj, Training feedforward networks with the Marquardt algorithm, IEEE Trans. Neural Netw., vol. 5, n.o 6, pp. 989-993, nov. 1994.
[28]M. A. Oskoei y H. Hu, Support Vector Machine-Based Classification Scheme for Myoelectric Control Applied to Upper Limb, *IEEE Trans. Biomed. Eng.*, vol. 55, n.º 8, pp. 1956-1965, ago. 2008.
[29]E. Kandel, J. Schwartz, y T. Jessell, *Principles of Neural Science*, 4 edition. New York: McGraw-Hill Medical, 2000.